Advances in Continuous and Discrete Models

RESEARCH Open Access

Risk contagion between global commodity and financial markets based on two-layer networks and SIS model

Yulian An[1*] and Yi Wang[1]

*Correspondence:
anyl@shisu.edu.cn
[1]School of Economics and Finance, Shanghai International Studies University, 1550 Wenxiang Road, Shanghai 201620, China

Abstract

With the deepening of commodity financialization, the risk linkage between global commodity markets and financial markets becomes more complex. In this paper, we investigate the risk interconnections between global financial markets and commodity markets in the context of commodity financialization, as well as the dynamic infectious process. To describe and analyze the risk contagion process between the two markets, we construct a two-layer spillover network for the mixed markets. Based on the network, we analyze the static average spillover risk and the dynamic spillover risk of different countries and commodities. Moreover, we propose an SIS epidemic model to discuss the dynamic contagion procession of spillover risk in the system. By focusing on five extreme events, we find that the basic reproduction number is great than 1 at all stages and has obvious change before and after these events. In this model, the cross-contagion rate parameters between two markets can be positive or negative, indicating that the spillover risks between financial markets and commodity markets can both infect and hedge each other. This reflects the unique nature of financial risk contagion.

Keywords: Risk contagion; Financial markets; Commodity markets; Multi-layer networks; SIS model

1 Introduction

In the process of financialization of commodities, the connections between traditional financial markets and various commodity markets have become increasingly intricate, gradually forming a system in which a small disruption in any country's financial market or any commodity market can trigger widespread contagion, ultimately threatening the stability of the entire system [1–5]. Since the 2008 financial crisis, many black swan events and geopolitical conflicts have led to heightened global uncertainty, which severely impacts both commodity and financial markets [6–9]. Continuously monitoring the information in these markets and exploring their interconnections is of great importance for mitigating systemic financial risks.

Connectedness is essential for managing and measuring modern risks [4]. It quantifies the interdependence among system components, effectively integrating diverse risk di-

mensions into a unified measure [10]. Connectedness contains different metrics which can provide varied information. Among them, the net spillover index measures each element's net spillover capacity within the system, with positive values indicating risk sources and negative values indicating risk recipients. A large body of economic evidence indicates that there are significant information spillover effects and interlinkages between the international commodity markets and financial markets [11–14], with the impact of price fluctuations in energy commodities, precious metals, and agricultural products being particularly pronounced [15–17].

Diebold, Yılmaz [18] developed a network topology analysis method, employing connectedness as a network metric, which has been widely applied in risk research. In terms of the application of these financial spillover networks, most studies are limited to single-layer networks [19]. Single-layer networks have structural limitations, placing different markets at the same level and easily overlooking cross-market connections. In contrast, multi-layer networks can effectively incorporate the diverse information of complex systems along with their multi-layer structures [20]. In the current research on multi-layer financial networks, a number of studies use multiplex networks to investigate the different risk-connection channels within the same financial market, such as the interbank market [21], the collateral market [22], and the stock market [23]. Additionally, interdependent networks are more suitable for studying risks between different markets or countries, as they better highlight the connections across markets or nations [20].

The financial system is a complex chaotic system influenced by nonlinear dynamics, which traditional econometric methods and linear models fail to adequately capture [24]. Given the development of complex networks, researchers are turning to dynamic methods to investigate the dynamic characteristics of networks. Biondo et al. [25] proposed a multi-layer network with propagation dynamics, simulating the process of information dissemination and trading phases typical of financial markets. Due to the similarities in transmission mechanisms and dynamics between financial risks and infectious diseases, models from biological sciences are increasingly applied in financial research. Chen, Fan [26] proposed a SIS epidemic network model to describe the dynamics of the contagion process of liquidity crisis on the interbank lending network. Huang et al. [27] established a two-layer Granger network connecting the Chinese and U.S. stock markets through Hong Kong stock market, and constructed a SIR model to analyze the spread of financial shocks.

For spillover networks based on connectedness, many papers explored whether network structure is significantly affected by certain extreme events and macroeconomic factor [28]. In fact, in the dynamic net spillover network, the state of each node converts between being a risk receiver and a risk transmitter over time. This provides an opportunity to study the dynamic characteristics of the network using epidemic models. On the other hand, many existing researches focus on specific financial sub-markets, such as the stock market [29] or banking sector [30], and their relationships with commodity markets. However, a country's financial system includes various subsystems like the stock market, foreign exchange market, and interbank market, a single index cannot adequately represent the overall financial condition.

Motivated by these studies, in this paper, we investigate the risk interconnections between global financial markets and commodity markets in the context of commodity financialization, as well as the dynamic infectious process. Firstly, we establish a financial stress index for each country with a standardized approach proposed by Illing, Liu [31],

which characterizes a country's financial risk situation from multiple dimensions. According to Adhikari, Putnam [2], the index can quantify systemic financial stress and identify disruptions in the normal functioning of financial markets. The index value is normalized so that a value of zero indicates normal financial stress levels. A positive value signifies above-average stress levels, while a negative value indicates below-average stress levels. In commodity markets, we utilize the indicator of commodity returns, which is commonly used in related studies [7, 32, 33]. Then, a two-layer network is constructed based on the approach of Diebold, Yilmaz [34]. Secondly, the dynamic net spillover index of risk is calculated using a rolling window method. Then, an SIS model is developed based on the two-layer network to examine the dynamic evolution of the net spillover index of risk before and after five extreme events. We focus on the variations in the overall risk contagion capability of the whole system, including both financial and commodity markets, during each event period.

The rest of this paper is organized as follows. Section 2 focuses on the selection of financial data from various countries and global commodity data. Section 3 discusses the methods employed, primarily emphasizing the VAR approach, the building of two-layer network and the SIS model. An empirical result and the variations in risk contagion capacity before and after five extreme events are given in Sect. 4 and Sect. 5. Finally, we give a conclusion in Sect. 6.

2 Data

The data is sourced from *Investing.com*. This database is a free financial data platform that provides real-time data from 250 exchanges worldwide (daily, monthly, and annually), along with quotes, charts, breaking news, and analysis, available in 44 language versions.

The sample period spans from January 10, 2007 to December 29, 2023, which includes a series of significant events such as the 2008 financial crisis, the 2014 oil price decline, the 2018 U.S.–China trade war, the COVID-19 pandemic in 2020, and the Russia–Ukraine war in 2022. A total of 4272 sample values are obtained after processing the data.

First, we select 15 countries from the top 20 nations ranked by total GDP in the World Bank's 2022 report, depending on data availability. The chosen countries are the United States, China, Japan, Germany, India, the United Kingdom, France, Russia, Brazil, Australia, South Korea, Mexico, Indonesia, Saudi Arabia, and Turkey, representing five continents: Asia, North America, South America, Europe, and Oceania. These nations are globally representative due to their substantial economic output, which constitutes a significant portion of global GDP, thus influencing international markets. Additionally, these economies host the world's major financial centers, playing a crucial role in global capital flows. Moreover, among these countries, some are clearly resource-consuming nations (such as the United States, China and Japan), while others are prominent resource-exporting countries (like Russia, Brazil, and Saudi Arabia). Their production and consumption behavior serve as fundamental determinants in the commodity markets. Subsequently, drawing on the methodology by Balcilar et al. [28] for constructing a financial stress index (FSI) for 11 countries, we select stock market indices, banking or financial indices, and exchange rates for 15 countries, as shown in Table 1, to construct the financial stress index for each country using the variance-equal weighted approach.

This method is simple to compute and accurately scales financial stress, making it widely adopted in many studies [31, 35, 36]. Indicators are selected from the banking sector, stock market, and foreign exchange market as follows:

Table 1 Financial data sources table

No.	Country	Stock	Bank	Foreign Exchange
1	US	S&P 500	KBW	DXY
2	CHN	CSI 300	CSI Bank	USD/CNY
3	JP	TOPIX	TOPIX Banks	USD/JPY
4	GER	DAX 30	DAX Banks	EUR/USD
5	IND	Nifty 50	Nifty Bank	USD/INR
6	GBR	FTSE 100	FTSE 350 Banks	GBP/USD
7	FRA	CAC 40	CAC 40 Financials	EUR/USD
8	RU	MOEX	MOEX Financials	USD/RUB
9	BRA	IBOVESPA	IBOVESPA Financials	USD/BRL
10	AUS	ASX 200	ASX 200 Banks	AUD/USD
11	KOR	KOSPI	KRX Bank	USD/KRW
12	MEX	S&P/BMV IPC	S&P/BMV Financials	USD/MXN
13	IDN	IDX	IDX Finance	USD/IDR
14	SA	TASI	TASI Bank	USD/SAR
15	TUR	BIST 100	BIST Banks	USD/TRY

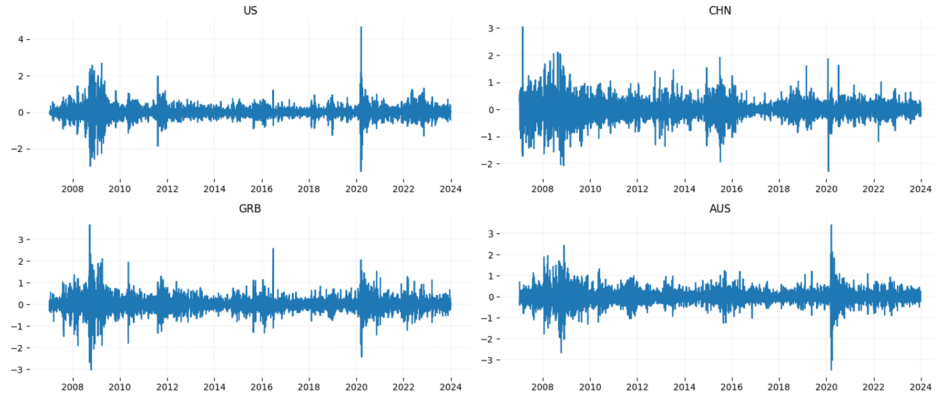

Figure 1 First difference of financial stress index (FSI) for countries

i) The banking sector consists of three main variables: systemic risk of banks (calculated using a 60-day rolling window with the standard Capital Asset Pricing Model (CAPM)), the negative returns of the banking index, and the volatility of the banking index.

ii) The stock market includes two variables: negative stock returns and the volatility of the stock index.

iii) In the foreign exchange market, the volatility of the currency is selected.

Due to a negative value in the original form, FSI data have been taken in the first difference [7].

Figure 1 displays the time series plots of the first difference of FSI series for the first 4 countries we study, with the remaining countries presented in Appendix A as Fig. 1 (continued).

In terms of commodity selection, we chose ten basic commodities: gold, silver, copper, aluminum, nickel, oil, natural gas, wheat, corn, and soybeans, using their daily closing prices in futures, as shown in Table 2. These commodities hold significant positions in the global market and have a substantial impact on the global economy.

We use the logarithmic returns of commodity prices, calculated as follows:

$$R_{i,t} = \ln\left(\frac{P_{i,t}}{P_{i,t-1}}\right). \tag{1}$$

Table 2 Commodity data sources table

Category	Commodity	Code
Precious Metals	Gold (NYMEX)	Gold
	Silver (NYMEX)	Silver
Industrial Metals	Copper (LME)	Copper
	Aluminum (LME)	Aluminum
	Nickel (LME)	Nickel
Energy	WTI Crude Oil (NYMEX)	WTI
	Natural Gas (CME)	Ngas
Grains	Wheat (CBOT)	Wheat
	Corn (CBOT)	Corn
	Soybean (CBOT)	Soybean

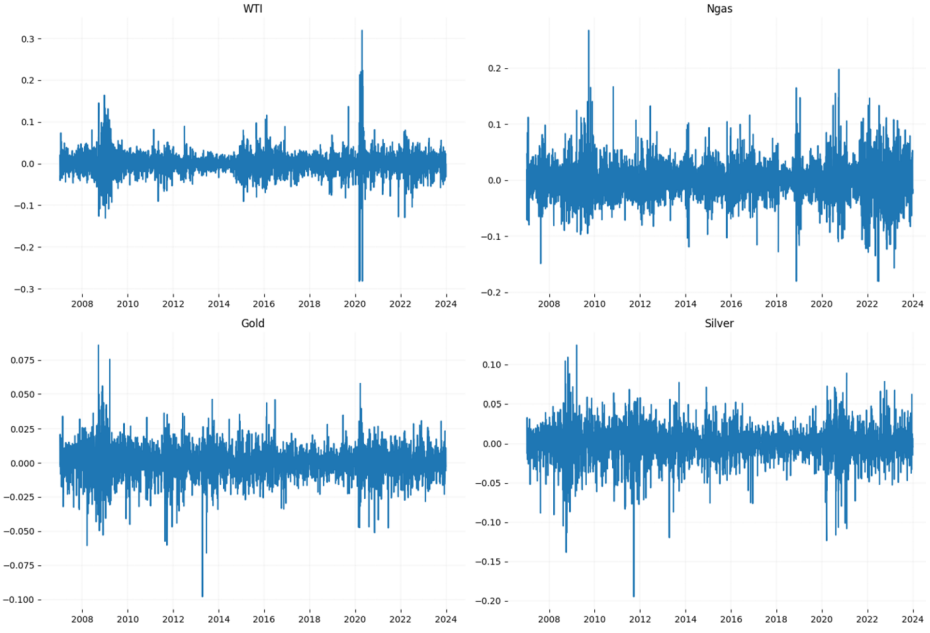

Figure 2 Logarithmic returns of commodity prices of oil, natural gas, gold, and silver prices

Here, $P_{i,t}$ is the closing price of the ith commodity on day t. Figure 2 presents the logarithmic returns of oil, natural gas, gold, and silver prices, while the returns of the remaining commodities are provided in Fig. 2 (continued) in Appendix A. These time series all pass the stationarity test.

3 Methods

In the section, we first construct a two-layer net spillover network for financial markets and commodity markets, using the standard VAR model (Diebold, Yilmaz [34]). Second, we establish an SIS model to describe the dynamic risk propagation process between two markets. Third, we calculate the basic reproduction number of the SIS model before and after five extreme events.

3.1 Connectedness measurement

Consider a N-variable covariance stationary VAR(p) model defined as $X_t = V + \sum_{i=1}^{p} \Phi_i X_{t-i} + \varepsilon_t$, Φ_i are $N \times N$ coefficient matrix, and ε_t is a normally distributed white

noise error term, $\varepsilon_t \sim (0, \Sigma)$, V is the N-dimensional intercept vector. Using the Wold decomposition theorem, the model can be transformed into the moving average representation given by $X_t = Z + \sum_{i=0}^{\infty} A_i \varepsilon_{t-i}$, where A_i denote $N \times N$ coefficient matrices following the recursion $A_i = \sum_{j=1}^{p} \Phi_j A_{t-j}$. Then we perform generalized forecast error variance decomposition, which is invariant to the variable ordering [34]. The H-step-ahead generalized forecast error variance for ith variable can be written as

$$\theta_{ij}^{g}(H) = \frac{\sigma_{jj}^{-1} \sum_{h=0}^{H-1} \left(e_i' A_h e_j\right)^2}{\sum_{h=0}^{H-1} \left(e_i' A_h C A_h' e_i\right)}, \tag{2}$$

where C denotes the covariance matrix of errors, σ_{jj} denotes the standard deviation of the disturbance term in the *jth* equation, and e_i denotes the selection vector. Due to the fact that the forecast error variance contributions may not be equal to 1, standardization is required as follows:

$$\tilde{\theta}_{ij}^{g}(H) = \frac{\theta_{ij}^{g}(H)}{\sum_{j=1}^{N} \theta_{ij}^{g}(H)}. \tag{3}$$

Thus, the sum of the variance decompositions in individual market, including own shocks, equals one, or $\sum_{j=1}^{N} \tilde{\theta}_{ij}^{g}(H) = 1$, and the sum of the total variance decompositions in all markets equals $\sum_{i,j=1}^{N} \tilde{\theta}_{ij}^{g}(H) = N$.

Then, by transforming $\tilde{\theta}_{ij}^{g}(H)$ to a directional spillover from country i to country j, we obtain the connectedness matrix:

$$S = \begin{bmatrix} 0 & \tilde{\theta}_{21}^{g} & \cdots & \tilde{\theta}_{N1}^{g} \\ \tilde{\theta}_{12}^{g} & 0 & & \tilde{\theta}_{N2}^{g} \\ \vdots & & \ddots & \vdots \\ \tilde{\theta}_{1N}^{g} & \tilde{\theta}_{2N}^{g} & \cdots & 0 \end{bmatrix}. \tag{4}$$

Next, we obtain three directional connectedness (risk spillover effect) measures. The first is total directional connectedness from i to other markets, which is defined as

$$C_{i\rightarrow\cdot}^{g}(H) = \sum_{j=1, j\neq i}^{N} \tilde{\theta}_{ij}^{g}(H). \tag{5}$$

The second is total directional connectedness from other markets to market i, which is

$$C_{i\leftarrow\cdot}^{g}(H) = \sum_{j=1, j\neq i}^{N} \tilde{\theta}_{ji}^{g}(H). \tag{6}$$

The third is net total directional connectedness, which is

$$C_{i}^{g}(H) = C_{i\rightarrow\cdot}^{g}(H) - C_{i\leftarrow\cdot}^{g}(H). \tag{7}$$

Besides, we also obtain total connectedness index (TCI), which is

$$TCI = \frac{1}{N} \sum_{i=1}^{N} \sum_{j=1, j\neq i}^{N} \tilde{\theta}_{ij}^{g}(H). \tag{8}$$

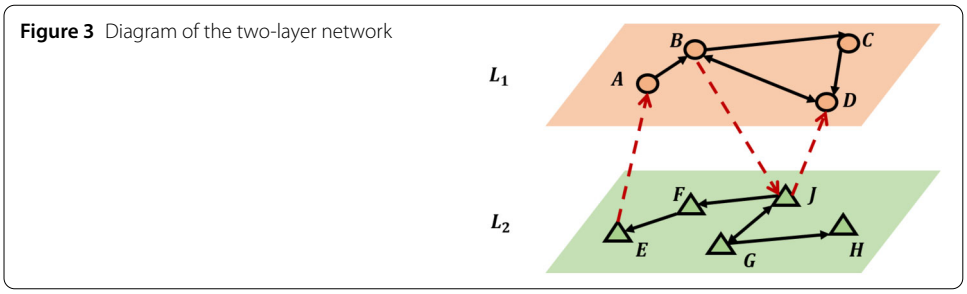

Figure 3 Diagram of the two-layer network

To alleviate the curse of dimensionality, we chose the LASSO-VAR model [37], incorporating a penalty term in the regression to complete parameter estimation and variable selection.

3.2 Network

3.2.1 Network structure

A two-layer spillover network is constructed for global commodity and financial markets based on connectedness table, as shown in Fig. 3. Nodes A, B, C, and D in layer L_1 constitute a commodity market, while nodes E, F, G, H, and J in layer L_2 form an international financial market. Within each layer and between layers, if there is a risk spillover effect between two nodes, there exists a corresponding edge between them. The two-layer network features both intra-layer and inter-layer structures. For example, the edge between internal nodes A and B in L_1 represents the connection between commodity markets A and B, the edge between internal nodes E and F in L_2 signifies the connection between the financial markets of countries E and F, and the edge between A and E represents the risk spillover relationship between commodity market A and the financial market of country E.

3.2.2 Network centrality measures

This study examines two different network centrality measurements. The degree centrality is a simple network analysis metric that simply counts the number of links that a node has. The bidirectional network is divided into in-degree centrality and out-degree centrality. For a node v_i, the in-degree centrality is defined as: $C_{in}(v_i) = \sum_{j \neq i} A_{ji}$, where A_{ji} indicates the existence of an edge from node v_j to node v_i. If the edge exists, then $A_{ji} = 1$; otherwise, $A_{ji} = 0$. The out-degree centrality is defined as: $C_{\text{out}}(v_i) = \sum_{j \neq i} A_{ij}$, where A_{ij} indicates the existence of an edge from node v_i to node v_j. If the edge exists, then $A_{ij} = 1$; otherwise, $A_{ij} = 0$.

Total degree centrality is the sum of in-degree centrality and out-degree centrality, reflecting a node's overall connectivity within the network. Total degree centrality is defined as:

$$C_{total}(v_i) = C_{in}(v_i) + C_{out}(v_i). \tag{9}$$

PageRank centrality evaluates the importance of nodes based on their connections and link quality, helping to identify key financial markets and their interdependencies, which is defined as:

$$PR_v = \gamma \sum_{u \epsilon B_v} \frac{PR_u}{N_u} + (1 - \gamma), \tag{10}$$

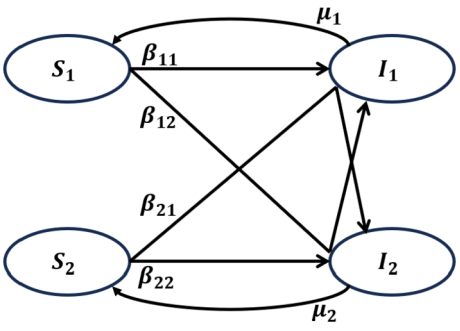

Figure 4 Sketch of risk spreading on the two-layer network

where PR_v represents the PageRank centrality of node v, B_v is the set of nodes pointing to node v, N_u is the number of edges originating from node u, and $\gamma \in [0,1]$ is the damping factor. In practice, we consider the more general setting in which $\gamma = 0.85$, a setting that is typical of PageRank algorithm.

3.3 SIS epidemic model

An epidemic model is constructed based on the aforementioned interconnected two-layer network. Each node has only two states: infected (I) and susceptible (S), and can transition between these two states, following the Susceptible-Infected-Susceptible (SIS) model. The entire infection process can be described as follows: The initial infected node can appear anywhere. Then, at each time step, if a susceptible node in L_1 is connected to an infected node in L_1, it will be infected at a rate of β_{11}; if it is connected to an infected node in L_2, it will be infected at a rate of β_{21}. If a susceptible node in L_2 is connected to an infected node in L_2, it will be infected at a rate of β_{22}; if it is connected to an infected node in L_1, it will be infected at a rate of β_{12}. Additionally, the probabilities of recovery for infected nodes in networks L_1 and L_2 are μ_1 and μ_2, respectively. This infection process is illustrated in Fig. 4.

Let S_1 and S_2 represent the number of susceptible nodes in networks L_1 and L_2, respectively, and I_1 and I_2 denote the number of infected nodes. The modified SIS model is as follows:

$$\begin{cases} \frac{dI_1}{dt} = \beta_{11} k S_1 I_1 / N_1 + \beta_{21} m S_1 I_2 / N_2 - \mu_1 I_1 \\ \frac{dI_2}{dt} = \beta_{22} l S_2 I_2 / N_2 + \beta_{12} m S_2 I_1 / N_1 - \mu_2 I_2 \\ S_1 + I_1 = N_1 \\ S_2 + I_2 = N_2 \end{cases} \tag{11}$$

Here, k, l, m represent the degree in layer L_1, L_2, and the intermediate layer, respectively. According to Huang et al. [27], for the convenience of subsequent differentiation and calculation, the mean degree $\langle k \rangle$, $\langle l \rangle$, $\langle m \rangle$ are used to replace k, l, m:

$$\langle k \rangle = \sum_{i=1}^{M_1} i p_1(i), \qquad \langle l \rangle = \sum_{i=1}^{M_2} i p_2(i), \qquad \langle m \rangle = \sum_{i=1}^{M_3} i p_3(i). \tag{12}$$

Here, M_1, M_2, M_3 represent the maximum degrees in layers L_1, L_2 and the intermediate layer, respectively, while p_1, p_2 and p_3 denote the degree distributions of layers L_1, L_2 and

the intermediate layer. N_1 and N_2 are the total number of nodes in networks L_1 and L_2, respectively.

In general, the parameters β_{11}, β_{22}, μ_1, μ_2 are nonnegative. However, the estimated parameters β_{21} and β_{12} can be negative or positive. A positive cross-market infection rate indicates a positive risk transmission relationship between the financial and commodity markets. Conversely, if β_{21} or β_{12} is negative, it suggests the self-protection of another node when a risk occurs at one node, such as hedging relationship found in previous studies [38, 39].

3.4 Parameter and basic reproduction number estimation

R_0 is a crucial indicator in epidemic models used to measure the transmission potential of infectious diseases [40]. It indicates the average number of secondary infections generated by one infected individual throughout their entire infectious period, in the absence of any interventions. If $R_0 > 1$, it indicates that the disease is spreading, while $R_0 < 1$ suggests that the disease is gradually disappearing and the system is stabilizing.

According to Van den Driessche, Watmough [41], infected and uninfected compartments should be defined according to epidemiological principles. Therefore, I_1 and I_2 are regarded as infected compartments, while the others are considered non-infected compartments. Let

$$\mathcal{F} = \begin{pmatrix} \beta_{11} \langle k \rangle S_1 I_1 / N_1 + \beta_{21} \langle m \rangle S_1 I_2 / N_2 \\ \beta_{22} \langle l \rangle S_2 I_2 / N_2 + \beta_{12} \langle m \rangle S_2 I_1 / N_1 \end{pmatrix}, \qquad \mathcal{V} = \begin{pmatrix} \mu_1 I_1 \\ \mu_2 I_2 \end{pmatrix}, \tag{13}$$

where $\mathcal{F}$ and $\mathcal{V}$ represent the rate of new infections entering the compartments and the transfer of individuals out of the compartments, respectively.

From

$$F = \left[\frac{\partial \mathcal{F}_i}{\partial x_j} \right], \qquad V = \left[\frac{\partial \mathcal{V}_i}{\partial x_j} \right], \tag{14}$$

where x_i are the compartments of model (11), defined as

$$x = (I_1, I_2, S_1, S_2)^T. \tag{15}$$

$m = 2$ is the number of infected compartments in model (11), $1 \le i, j \le m$. Then, we give 2×2 Jacobi matrix F and V at disease-free equilibrium

$$F = \begin{pmatrix} \beta_{11} \langle k \rangle & \beta_{21} \langle m \rangle N_1 / N_2 \\ \beta_{12} \langle m \rangle N_2 / N_1 & \beta_{22} \langle l \rangle \end{pmatrix} \tag{16}$$

$$V = \begin{pmatrix} \mu_1 & 0 \\ 0 & \mu_2 \end{pmatrix}. \tag{17}$$

Consequently, the basic reproduction number here is

$$R_0 = \rho \left(F V^{-1} \right), \tag{18}$$

where $\rho(A)$ denotes the magnitude of spectral radius of a matrix A [41].

The parameters of model (11) are estimated using the least squares method and numerical simulation from the dynamic net spillover index. First, in terms of market state classification, the net spillover index obtained from the LASSO-VAR connectedness method allows for the categorization of each market as either a spillover source or a spillover recipient. If a market has a net spillover index greater than 0, it is classified as infected (I); if the index is less than 0, the market is categorized as susceptible (S). Secondly, the objective is to minimize the sum of squared distances:

$$\mathbf{min}\, E = \sum_{i=1}^{n} \left[\left(S_i - \hat{S}_i \right)^2 + \left(I_i - \hat{I}_i \right)^2 \right], \tag{19}$$

where S_i, I_i are the true number of susceptible nodes and infected nodes respectively, and $\hat{S}_i$, $\hat{I}_i$ are the corresponding numbers from numerical simulation. n is the number of observing days in some time segment.

4 Empirical results

4.1 Full sample two-layer network

During the sample period, the connectedness table over the full sample period is obtained according to equation (2), as shown in Table 3. From Table 3, we can find that the total connectedness accounts for 52.52 % of the total forecast-error variance. It indicates that those markets are highly interconnected where more than half of the total forecast error variance can be attributed to the connectedness across the 25 nodes. Now, we construct a two-layer network based on the connectedness Table 3. To reduce noise and information redundancy and maintain consistency in network analysis across different periods, we only chose the top 25% of edge weights to build network. Thus, Fig. 5 illustrates the two-layer network constructed from the full sample. L_1 represents the commodity market layer, L_2 represents the financial market layer. Especially, the cross-market layer is shown in Fig. 6. During the full sample, the clustering results divide the network into five clusters by using the Louvain algorithm, which can detect community structure by optimizing network modularity [42].

The financial markets are split into two clusters: Cluster 1 (orange) includes the U.S., the U.K., France, Germany, Mexico, Brazil, Turkey, Russia, and Saudi Arabia, while Cluster 2 (green) consists of China, South Korea, Japan, Australia, India, and Indonesia. This division shows a strong regional pattern, with Cluster 1 primarily comprising markets from Europe and the Americas, and Cluster 2 from Asia and Oceania. The commodity markets are grouped into three clusters: Cluster 3 (purple) includes silver, gold, crude oil (WTI), copper, aluminum, and nickel; Cluster 4 (blue) consists of corn, soybeans, and wheat; and natural gas forms an independent Cluster 5 (gray).

Table 4 presents the degree centrality and PageRank rankings for the entire sample period. In the degree centrality ranking, the UK, France, and Germany occupy the top three positions, indicating that these major European financial centers have high direct connectivity and serve as primary risk aggregation centers. Copper and oil (WTI) also exhibit high degree centrality in the commodity market, marking them as key risk assets globally. According to the PageRank rankings, South Korea, Australia, and Indonesia rank among the top five in financial markets, highlighting their significant roles in the Asia–Pacific region and global risk transmission. In the commodity market, corn and silver are notably

Table 3 Overall connectedness based on a LASSO-VAR model

	US	CHN	GRB	AUS	BRA	GER	RU	FRA	KOR	MEX	JP	SA	TUR	IDN	IND	WTI	Ngas	Gold	Silver	Wheat	Corn	Soybean	Copper	Aluminum	Nickel	FROM
US	29.75	0.22	8.98	1.89	9.59	10.23	1.23	10.22	1.28	12.31	1.19	1.08	2.22	0.71	1.62	2.21	0.12	0.01	0.24	0.29	0.23	0.51	2.06	1.15	0.65	70.25
CHN	0.55	72.18	1.36	2.99	1.11	0.91	0.39	1.01	5.73	0.68	2.48	0.29	0.35	3	2.51	0.52	0	0.02	0.25	0.04	0.15	0.47	1.97	0.55	0.49	27.82
GRB	6.46	0.48	23.88	2.24	4.03	15.59	2.12	17.29	1.86	5.29	1.79	0.94	3.89	1.23	2.49	1.88	0.04	0.03	0.5	0.22	0.36	0.81	3.92	1.55	1.12	76.12
AUS	5.64	2.04	4.32	46.1	2.72	4.32	0.54	4.33	7.46	4.18	5.16	1.52	1.19	3.38	3.38	0.7	0.03	0.08	0.33	0.11	0.1	0.35	1.16	0.46	0.4	53.9
BRA	11.38	0.58	6.38	1.77	35.22	6.9	1.51	7.01	1.73	10.49	1.05	1.27	2.16	1.11	2	2.36	0.09	0.13	0.58	0.45	0.63	0.95	2.4	0.9	0.95	64.78
GER	7.39	0.32	15.15	1.91	4.39	23.49	1.9	19.74	1.83	5.73	1.43	1.05	3.29	0.94	2.4	1.61	0.04	0.01	0.45	0.18	0.29	0.75	3.42	1.45	0.86	76.51
RU	2.26	0.32	4.97	0.71	2.38	4.57	58.45	5.14	1.3	2.69	0.99	0.94	3.17	0.91	1.17	1.7	0.11	0.11	0.67	0.68	0.81	0.85	2.3	1.26	1.53	41.55
FRA	7.04	0.34	16.11	1.93	4.26	18.99	2.06	23.18	1.57	5.59	1.48	0.93	3.51	1.16	2.54	1.57	0.05	0.01	0.4	0.19	0.27	0.73	3.69	1.46	0.95	76.82
KOR	3.38	3.5	3.44	7.68	2.56	3.6	0.92	3.44	45.34	2.54	7.61	1.4	1.32	4.36	4.31	0.66	0.02	0.07	0.37	0.05	0.08	0.53	1.75	0.66	0.41	54.66
MEX	13.43	0.31	8.02	1.36	9.6	8.51	1.55	8.85	1.55	32.28	0.79	0.9	2.37	0.9	1.4	1.57	0.12	0.06	0.57	0.34	0.36	0.73	2.41	1.07	0.95	67.72
JP	6	1.5	5	5.61	2.61	4.85	0.92	4.98	7.62	3.2	46.19	1.49	1.29	2.04	2.01	0.99	0.05	0.05	0.46	0.08	0.09	0.42	1.43	0.69	0.42	53.81
SA	2.35	0.28	2.66	2.8	2.34	3.04	1.1	2.88	2.35	1.82	2.35	67.47	1.21	1.29	1.42	1.32	0.24	0.01	0.32	0.16	0.15	0.67	0.64	0.62	0.49	32.53
TUR	3.5	0.25	7.6	1.44	2.94	6.89	2.72	7.62	1.59	3.39	1.07	0.89	50.31	1.62	2.33	0.74	0.06	0.16	0.66	0.12	0.3	0.47	1.82	0.61	0.89	49.69
IDN	2.21	2.35	2.87	4.68	1.94	2.36	0.89	3.04	5.83	1.89	2.63	1.07	1.8	57.18	5.98	0.62	0.01	0.11	0.97	0.03	0.05	0.18	0.91	0.28	0.13	42.82
IND	2.4	1.89	4.72	4.35	2.54	4.7	0.95	5.16	5.1	2.01	2.17	1	2.2	5.23	49.81	0.69	0.05	0.04	0.64	0.12	0.18	0.51	2	0.88	0.65	50.19
WTI	3.09	0.34	3.45	0.56	2.32	3.09	1.42	3.1	0.64	2.26	0.75	0.96	0.71	0.48	0.71	48.91	1.03	1.79	3.2	1.73	2.52	3.33	5.96	4.67	2.98	51.09
Ngas	0.32	0	0.12	0.04	0.2	0.15	0.17	0.17	0.01	0.34	0.08	0.32	0.11	0.01	0.1	1.92	91.55	0.16	0.43	0.56	0.96	0.6	0.52	0.9	0.26	8.45
Gold	0.01	0.01	0.01	0.09	0.14	0	0.1	0.01	0.07	0.09	0.05	0.01	0.16	0.1	0.05	1.89	0.09	51.55	32.75	1.08	1.28	1.41	3.95	3.08	2.03	48.45
Silver	0.26	0.14	0.7	0.36	0.6	0.68	0.49	0.58	0.38	0.7	0.42	0.2	0.54	0.73	0.57	2.81	0.2	27.29	42.95	1.21	1.74	2.33	6.32	4.72	3.08	57.05
Wheat	0.49	0.03	0.46	0.12	0.66	0.39	0.67	0.43	0.01	0.58	0.03	0.14	0.13	0.02	0.15	2.04	0.35	1.2	1.62	57.67	19.37	8.75	2.05	1.69	0.94	42.33
Corn	0.34	0.1	0.69	0.09	0.83	0.57	0.72	0.54	0.07	0.55	0.04	0.12	0.3	0.04	0.2	2.66	0.54	1.28	2.09	17.4	51.78	13.57	2.34	1.93	1.2	48.22
Soybean	0.73	0.32	1.51	0.43	1.21	1.45	0.73	1.45	0.64	1.07	0.41	0.49	0.46	0.15	0.54	3.42	0.33	1.38	2.73	7.62	13.16	50.23	4.34	3.1	2.13	49.77
Copper	1.93	0.89	4.54	0.86	2.11	4.2	1.34	4.54	1.41	2.31	0.81	0.32	1.16	0.52	1.41	4.16	0.19	2.61	5.02	1.21	1.54	2.95	34.11	11.68	8.15	65.89
Aluminum	1.4	0.32	2.38	0.36	0.96	2.23	0.97	2.33	0.68	1.33	0.51	0.41	0.5	0.2	0.82	4.29	0.44	2.69	4.94	1.32	1.67	2.77	15.39	44.94	6.15	55.06
Nickel	0.94	0.34	2.05	0.48	1.27	1.61	1.38	1.83	0.49	1.44	0.37	0.38	0.9	0.1	0.72	3.2	0.15	2.07	3.76	0.86	1.21	2.22	12.54	7.18	52.5	47.5
TO	83.5	16.87	107.53	44.75	63.31	109.84	26.79	115.71	51.2	72.48	35.64	18.13	34.93	30.25	40.81	45.54	4.35	41.38	63.94	36.03	47.52	46.85	85.28	52.56	37.8	**52.52**
NET	13.25	−10.96	31.4	−9.16	−1.48	33.33	−14.76	38.89	−3.45	4.76	−18.17	−14.4	−14.76	−12.58	−9.38	−5.56	−4.09	−7.07	6.89	−6.3	−0.7	−2.92	19.4	−2.5	−9.7	

Note: The table reports the generalized connectedness measures estimated using the approach of Diebold and Yilmaz (2012). The lag order of the LASSO-VAR models is 2 and was selected using the Bayesian information criterion (BIC). Bold denotes the total connectedness index.

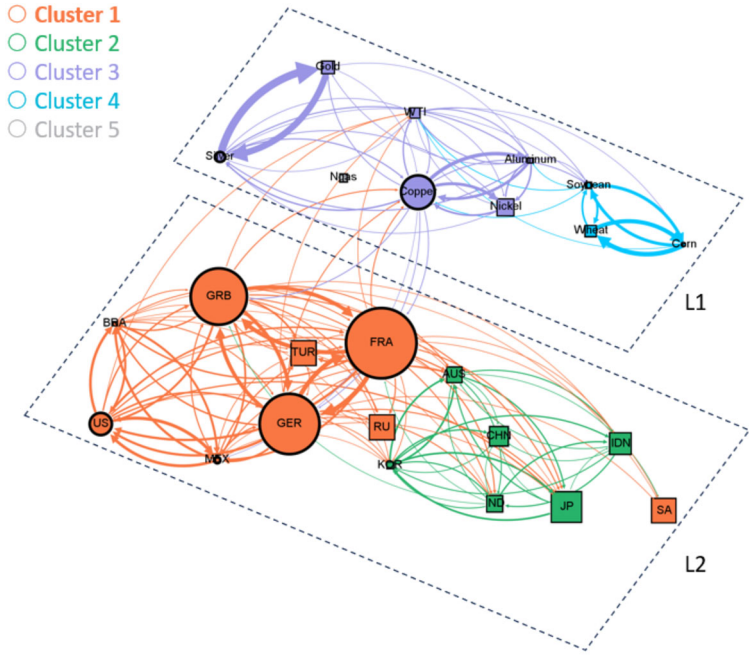

Figure 5 Full sample two-layer network. *Note:* The network is based on LASSO-VAR. Node shape indicates node net overflow state, circle indicates positive net overflow, square indicates negative net overflow. The node size is proportional to the net overflow strength. The color of the node indicates the cluster group. The thickness of the edge is proportional to the directional overflow strength of each node

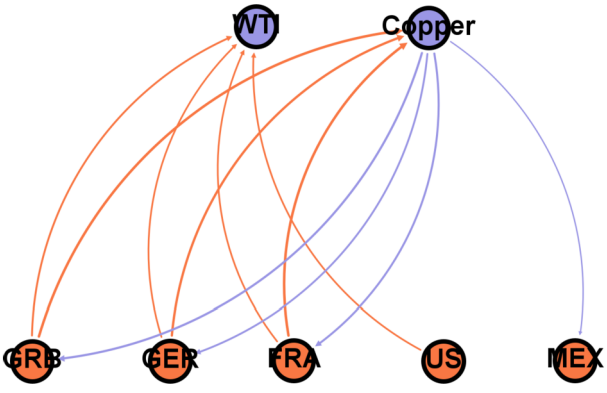

Figure 6 The cross-market layer of the full sample two-layer network

Table 4 Full sample network statistics

Rank	Full sample	
	Degree centrality	PageRank
1	FRA	KOR
2	GRB	AUS
3	GER	Corn
4	Copper	Silver
5	WTI	IDN

Table 5 Full sample network's character statistics

Layer	Edges	Average degree	Network diameter	Graph density	Average path length
Financial	98	6.533	4	0.467	1.801
Commodity	41	4.1	3	0.456	1.528
Intermediate	11	1.571	2	0.262	1.467

influential within the network. South Korea, Australia, and Indonesia, as major economies in the Asia–Pacific region, play a critical role in international financial markets. Corn, as a primary food crop, is also widely used in animal feed and biofuel production, while silver possesses both industrial and investment value. They all serve as key nodes in risk transmission.

In the cross-market layer shown in Fig. 6, oil and copper play important roles. Oil (WTI) primarily absorbs risk spillover from developed country financial markets, while copper's interactions with financial markets involve both risk spillover and risk absorption.

Table 5 presents the structural statistics of the network layers. The financial market layer contains 98 connections, with an average of 6.533 connections per node, a network density near 0.5, and an average path length of less than 2, indicating dense connections and rapid information transmission. In the commodity layer, there are 41 connections and an average of 4.1 connections per node, with a network density of 0.456, suggesting sparser connections compared to the financial layer. However, the commodity layer has a smaller network diameter and average path length, indicating faster and more efficient information and risk transmission among commodity markets. In the cross-market layer, despite fewer connections, both the network diameter and average path length suggest quick risk transmission between markets.

4.2 Calculating the dynamic net total directional connectedness

The static spillover analysis provides interesting and useful insights on the average financial connectedness among the markets over the entire sample period. However, it masks important information on the dynamic evolution of the connectedness pattern over time. To this end, we use the sliding window method to calculate the dynamic net total directional connectedness for mixed markets. The parameters are set as follows: the window width ω is 200 days, the lag order p of the VAR is 2 days based on the Bayesian Information Criterion (BIC), and the forecast period H is 10 days.

4.2.1 Individual dynamic overflow

At the micro-individual level, using equation (7) and rolling window methods, we can obtain the dynamic net total directional connectedness for each market. Figure 7 and Fig. 8 present heatmaps for dynamic net total directional connectedness in the financial and commodity markets, respectively. Deep blue indicates a negative net intensity, representing net recipients of spillover effects; green to red indicates a positive net intensity, representing net sources of spillover effects. During the sample period, the financial markets of France, Germany, the UK, and the US were almost always net sources of spillover effects, while the remaining financial markets predominantly acted as net recipients of spillover effects. Between 2008 and 2014, the net spillover capacity of copper, aluminum, silver, and crude oil significantly increased, while the spillover resilience of gold and natural gas also improved during this period. During the COVID-19 pandemic in 2020, all commodities in

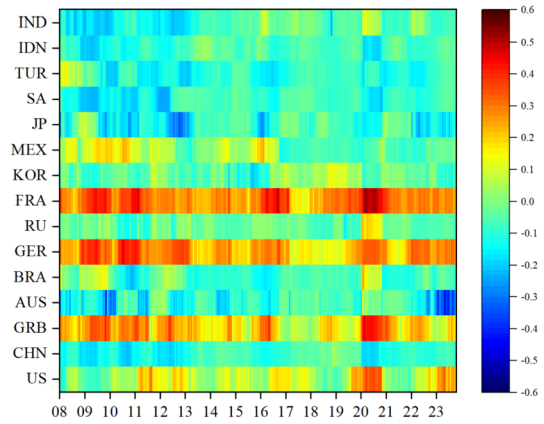

Figure 7 Dynamic net total directional connectedness in financial markets

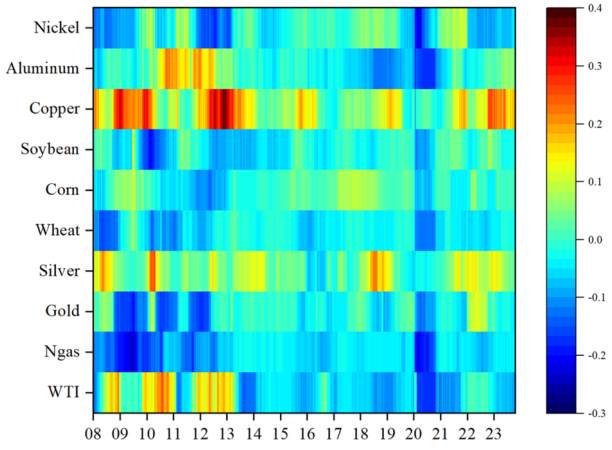

Figure 8 Dynamic net total directional connectedness in commodity markets

the commodity layer became net recipients of risk. However, during the Russia–Ukraine war, the net spillover capacity of copper and silver in the commodity layer was once again strengthened.

4.2.2 Cross-market dynamic overflow

Drawing on the methods of Wang (2023), we utilize block aggregation connectedness to directly analyze the spillover relationships between two markets. The core idea of this method is to sum and average all connectivity within the same market. Since the total spillover accepted by a market is 1, subtracting the market's internal spillover from 1 allows us to obtain the spillover from another market.

Figure 9 displays the dynamic block spillover index. The spillover effects within markets are significantly higher than those between markets. The internal spillover effects in financial markets are stronger than those in commodity markets, and the spillover from financial markets to commodity markets exceeds that from commodity markets to financial markets.

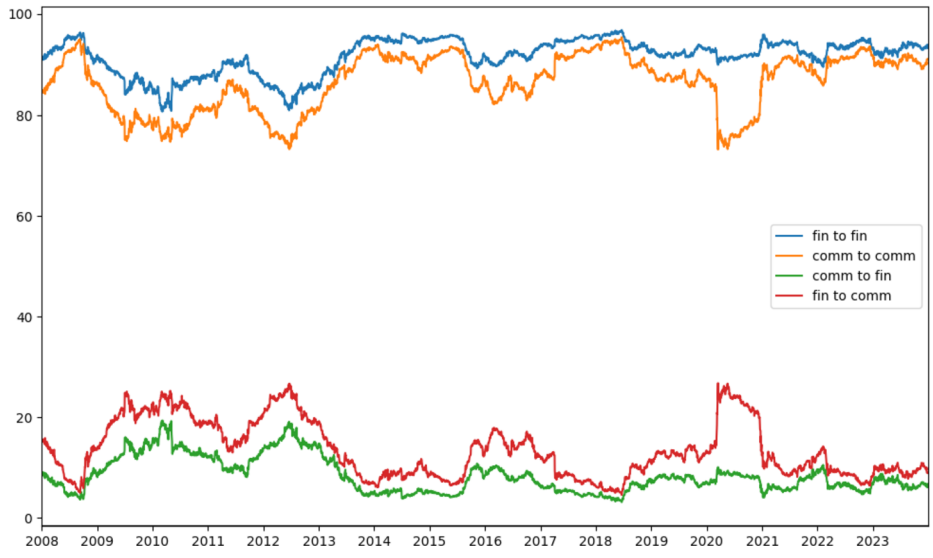

Figure 9 Block connectedness

5 The variations in risk contagion capacity before and after five extreme events

In this section, we select five significant events to study the changes in network structure before and after these events, and construct a two-layer epidemic model for each phase to explore the dynamic evolution of risk. The five events are: the bankruptcy of Lehman Brothers in 2008, the decline in oil prices in 2014, the outbreak of the U.S.–China trade war in 2018, the emergence of the COVID-19 pandemic in 2020, and the outbreak of the Russia–Ukraine war in 2022.

We select the 200-day window with an ending date of 15 September 2008 as the pre-collapse period, and another 200-day window ending on 11 December 2008 as the post-collapse period. In the second half of 2014, oil prices began to decline sharply. Therefore, we select the window with an ending date of 15 June 2014, as the pre-decline period for oil prices, and the window with an ending date of 12 January 2015, as the post-decline period. On March 22, 2018, the United States announced tariffs on China. Thus, the window with an ending date of 22 March 2018 is regarded as the pre-trade war period, and the window with an ending date of 24 September 2018 as the post-trade war period. For the COVID-19 pandemic, the window up to January 23, 2020, is designated as pre-pandemic, while up to May 4, 2020, serves as post-pandemic. Following the outbreak of the Russia–Ukraine war on February 24, 2022, the window up to February 24, 2022, is chosen as the pre-war period, and the window up to June 23, 2022, is selected as the post-war period. Each window is 200 days long, providing a sufficiently extended time series for a relatively stable network structure.

5.1 Constructing the global financial and commodity two-layer spillover network

We construct two-layer spillover networks for the periods before and after five extreme events. Figure 10 shows the networks before and after the bankruptcy of Lehman Brothers. In addition, the networks for the remaining four events are shown in Appendix B as Fig. 16-Fig. 19.

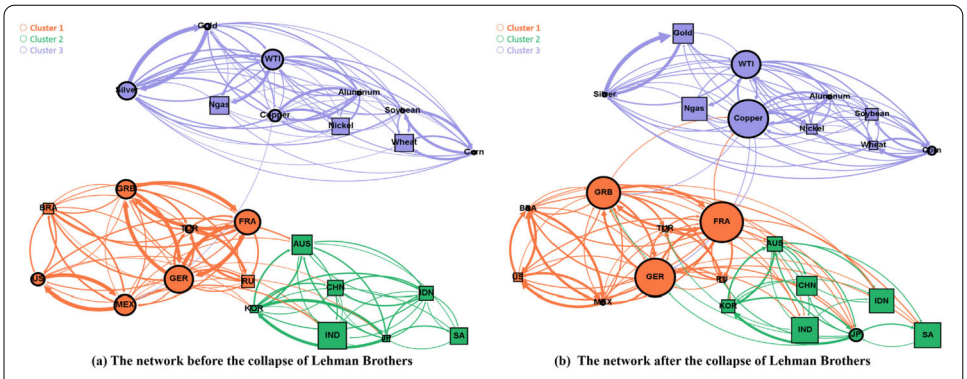

Figure 10 Two-layer networks before and after the bankruptcy of Lehman Brothers. *Note:* The network is constructed based on the LASSO-VAR model. Node shapes indicate net spillover status: circles for positive and squares for negative spillover. Node size is proportional to spillover strength, and color represents the cluster. Edge thickness reflects the directional spillover intensity

Table 6 Every network's characteristics statistics

	Layer	Edges	Average degree	Network diameter	Graph density	Average path length
Before event 1	Financial	82	5.467	4	0.39	1.643
	Commodity	62	6.3	2	0.7	1.3
	Intermediate	1	0.04	1	0.002	1
After event 1	Financial	82	5.467	4	0.39	1.765
	Commodity	62	6.2	2	0.689	1.311
	Intermediate	5	0.2	2	0.008	1.444
Before event 2	Financial	90	6	3	0.429	1.738
	Commodity	26	2.6	2	0.289	1.188
	Intermediate	27	1.08	6	0.045	2.077
After event 2	Financial	87	5.8	6	0.414	2.09
	Commodity	25	2.5	2	0.278	1.306
	Intermediate	31	1.24	7	0.052	2.723
Before event 3	Financial	100	6.667	4	0.476	1.629
	Commodity	31	3.1	2	0.344	1.262
	Intermediate	13	0.52	2	0.022	1.381
After event 3	Financial	92	6.133	4	0.438	1.662
	Commodity	32	3.2	2	0.356	1.111
	Intermediate	19	0.76	4	0.032	1.629
Before event 4	Financial	81	5.4	5	0.386	1.898
	Commodity	23	2.3	5	0.256	2.216
	Intermediate	40	1.6	6	0.067	2.52
After event 4	Financial	115	7.667	4	0.548	1.586
	Commodity	16	1.6	4	0.178	1.679
	Intermediate	18	0.72	3	0.03	1.771
Before event 5	Financial	84	5.6	4	0.4	1.905
	Commodity	34	3.4	3	0.378	1.444
	Intermediate	30	1.2	4	0.05	1.99
After event 5	Financial	78	5.2	4	0.371	1.714
	Commodity	52	5.2	2	0.578	1.278
	Intermediate	14	0.56	3	0.023	1.52

Note: Event 1 represents the bankruptcy of Lehman Brothers, Event 2 represents oil crisis, Event 3 represents the U.S.–China trade war, Event 4 represents the outbreak of COVID-19, and Event 5 represents the outbreak of the Russia–Ukraine war.

Table 6 displays every network's characteristics corresponding to these events. Before and after the bankruptcy of Lehman Brothers, the structure of financial and commod-

ity market layers experienced little change, but remained tightly connected. The commodity market exhibited higher average degree and graph density, along with lower network diameter and average path length, indicating stronger connectivity and a more compact structure, facilitating faster information transmission. After the bankruptcy, cross-market connections increased, with average degree and graph density rising compared to the pre-bankruptcy period, reflecting enhanced interactions between the financial and commodity markets following the crisis. After the decline in oil prices, the financial layer is comparatively sparse, with a graph density of 0.414 and a network diameter of 6. The commodity layer experienced a slight decrease in graph density, while the intermediate layer became slightly more compact but less efficient. During the period of the trade war, compared to the levels prior to its outbreak, the financial layer is comparatively sparse, with a graph density of 0.438, while the commodity layer is relatively dense, with a graph density of 0.356, indicating a slight weakening of connections in financial markets and a strengthening of connections in commodity markets. Besides, the intermediate layer also became slightly more compact, but less efficient. Compared to the pre-pandemic period, the financial layer becomes more compact, with a graph density of 0.548 and a relatively small network diameter. The commodity layer becomes relatively sparse, showing a decrease in graph density, while the intermediate layer exhibits higher density and a smaller diameter, indicating that cross-market connections have become more compact and risk transmission is significantly more efficient. After the Russia–Ukraine war, the financial market's graph density decreased, indicating reduced overall connectivity. In contrast, the commodity market experienced a significant increase in connections, with a higher graph density, and a decrease in network diameter and average path length, reflecting stronger interconnectivity than the financial market. Additionally, cross-market connections have decreased compared to the pre-war period.

Table 7 displays top five centrality of markets during these five events. It can be observed that the centrality rankings change after each event occurs. Generally, the financial markets of developed European countries such as France, Germany, and the UK are consistently at the core of risk accumulation, while oil (WTI) and copper typically serve as the central points of risk in the commodity market. The financial markets of South Korea and Australia, along with the corn commodity market, generally exhibit strong risk transmission capabilities.

5.2 Estimating parameters

The third step is to figure out the parameters and basic reproduction number of the SIS model. We select specific time points for these extreme events to study the conditions within a month before and after their occurrence. During the bankruptcy of Lehman Brothers, time segment 1 is defined as the pre-event period from August 18, 2008, to September 15, 2008, while time segment 2 spans from September 15, 2008, to October 15, 2008 as post-collapse period. In the oil crisis, time segment 1 is from May 9, 2014, to June 16, 2014, while time segment 2 is from June 16, 2014, to July 24, 2014. In the trade war, the pre-event period is from January 29, 2018, to March 7, 2018, and the post-event period is from March 7, 2018, to April 5, 2018. The pre-COVID-19 outbreak period is from December 13, 2019, to January 21, 2020, while the post-outbreak period is from January 21, 2020, to March 15, 2020. The pre-Russia-Ukraine war period is from January 13, 2022,

Table 7 The top five centrality of markets

Rank	Before event 1		After event 1	
	PageRank centrality	Degree centrality	PageRank centrality	Degree centrality
1	IDN	WTI	WTI	GRB
2	AUS	Silver	AUS	Copper
3	IND	MEX	JP	GER
4	KOR	Soybean	Silver	FRA
5	Corn	Gold	Copper	WTI
Rank	Before event 2		After event 2	
	PageRank centrality	Degree centrality	PageRank centrality	Degree centrality
1	KOR	GRB	JP	FRA
2	Silver	GER	Copper	GRB
3	JP	RU	Corn	US
4	Corn	TUR	AUS	IND
5	Copper	US	KOR	GER
Rank	Before event 3		After event 3	
	PageRank centrality	Degree centrality	PageRank centrality	Degree centrality
1	IND	FRA	Corn	GRB
2	KOR	GRB	KOR	FRA
3	AUS	GER	JP	CHN
4	FRA	IND	Wheat	JP
5	GER	KOR	Silver	GER
Rank	Before event 4		After event 4	
	PageRank centrality	Degree centrality	PageRank centrality	Degree centrality
1	KOR	US	KOR	FRA
2	Copper	Copper	Corn	GRB
3	JP	GER	IND	US
4	US	RU	CHN	GER
5	AUS	GRB	Wheat	IND
Rank	Before event 5		After event 5	
	PageRank centrality	Degree centrality	PageRank centrality	Degree centrality
1	Corn	GRB	IND	IND
2	JP	FRA	KOR	US
3	Soybean	GER	US	GER
4	KOR	WTI	Silver	FRA
5	Wheat	Copper	WTI	GRB

Note: Event 1 represents the bankruptcy of Lehman Brothers, Event 2 represents oil crisis, Event 3 represents the U.S.–China trade war, Event 4 represents the outbreak of COVID-19, and Event 5 represents the outbreak of the Russia–Ukraine war.

to February 23, 2022, while the post-war period is from February 23, 2022, to March 29, 2022.

Extract the net total directional connectedness sequences for each node from each time period and classify the infection status of each node according to the previously proposed method in Sect. 3, obtaining the values of S_i, I_i in equation (19). According to Table 6, before the bankruptcy, $\langle k \rangle = 6.3$, $\langle l \rangle = 5.467$, $\langle m \rangle = 0.04$; after the bankruptcy, $\langle k \rangle = 6.4$, $\langle l \rangle = 5.333$, $\langle m \rangle = 0.2$. The fitting results are shown in Fig. 11. Using numerical solution techniques, gain the numerical solution of SIS model (11) under the constraints of equation (19). The fitted parameters obtained of model (11) for pre-bankruptcy are

$$\left[\hat{\beta}_{11}, \hat{\beta}_{22}, \hat{\mu}_1, \hat{\mu}_2, \hat{\beta}_{12}, \hat{\beta}_{21}\right] = [0.0000,\ 0.4906,\ 0.2145,\ 1.0000,\ -14.9034,\ 29.0378].$$

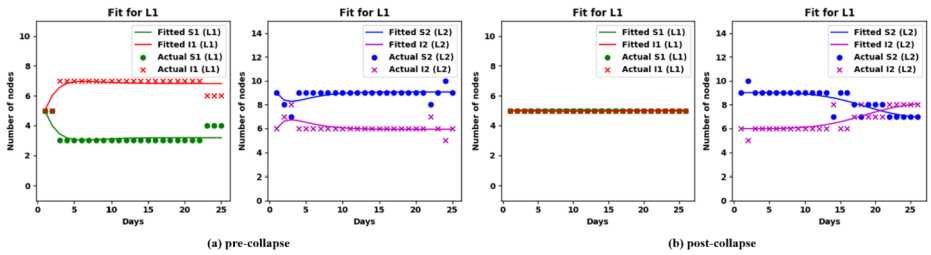

Figure 11 Parameters fitting for the model during the collapse of Lehman Brothers

The fitted parameters for post-bankruptcy are

$$\left[\hat{\beta}_{11}, \hat{\beta}_{22}, \hat{\mu}_1, \hat{\mu}_2, \hat{\beta}_{12}, \hat{\beta}_{21}\right] = [0.0913, 0.3391, 0.3021, 0.4902, -4.1657, 0.1992].$$

Before the bankruptcy of Lehman Brothers, the number of infections in the commodity market initially increased, then stabilized with a slight decline, while the internal infection rate approached zero and the external transmission rate was negative. In contrast, the infection count in the financial market remained generally stable, with an internal infection rate notably higher than that of the commodity market and a positive external transmission rate. This indicates that the commodity market primarily absorbs spillover risk from the financial market and acts as a hedge. Additionally, the external transmission rate being much higher than the internal rate suggests that transmission between markets is more rapid and frequent. After the bankruptcy of Lehman Brothers, the number of infections in the commodity market remained stable, with an increase in the internal infection rate, while the external transmission rate remained negative, but with a significant decrease in absolute value. In the financial market, showed an upward trend, with a slight decline in the internal infection rate compared to pre-collapse levels, though still higher than that of the commodity market, and a notable decrease in the external transmission rate, which remained positive. Additionally, the financial market's recovery rate declined significantly, while the commodity market's recovery rate improved. This indicates that post-collapse, a relationship of risk spillover and absorption persisted between the two markets, but the inter-market transmission rates were much lower than before the collapse. Internal transmission within the financial market was faster and more difficult to recover from compared to the commodity market.

According to Table 6, before the oil price decline $\langle k \rangle = 2.6$, $\langle l \rangle = 6$, $\langle m \rangle = 1.08$; after the decline, $\langle k \rangle = 2.5$, $\langle l \rangle = 5.8$, $\langle m \rangle = 1.24$. The fitting results are shown in Fig. 12.

The fitted parameters obtained before the decline in oil prices are:

$$[\hat{\beta}_{11}, \hat{\beta}_{22}, \hat{\mu}_1, \hat{\mu}_2, \hat{\beta}_{12}, \hat{\beta}_{21}] = [0.0000, 0.2647, 0.7786, 0.5657, -0.6639, 1.1386]$$

and those after the decline in oil prices are:

$$\left[\hat{\beta}_{11}, \hat{\beta}_{22}, \hat{\mu}_1, \hat{\mu}_2, \hat{\beta}_{12}, \hat{\beta}_{21}\right] = [0.8222, 0.0000, 0.9979, 0.0379, 0.0736, -0.4003].$$

In mid-2014, before the decline in oil prices, the number of infections in both the commodity and financial markets exhibited a generally stable trend. The internal infection rate

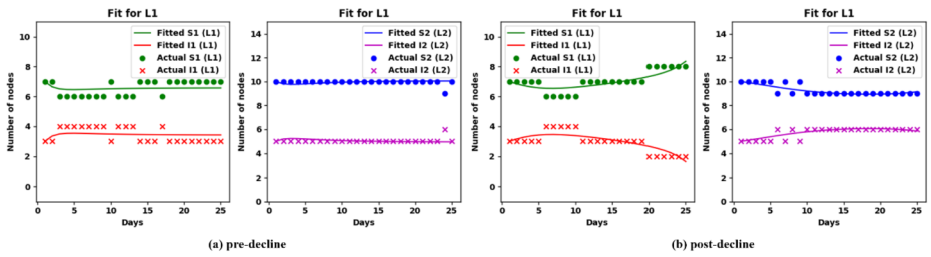

Figure 12 Parameters fitting for the model during the decline of oil prices

in the commodity market approached 0, with a negative external transmission rate; conversely, the internal infection rate in the financial market was significantly higher than that of the commodity market, and the external transmission rate was positive. This indicates that the commodity market was more susceptible to risk transmission from the financial market at that time, while also serving a hedging role against risks in the financial market. After the decline in oil prices, the number of infections in the commodity market initially rose and then fell, with both the internal infection rate and recovery rate significantly increasing, while the external transmission rate turned positive. In the financial market, the number of infections showed a slight upward trend, with a decrease in the internal infection rate and a shift in the external transmission rate to negative. This indicates that, at this time, the commodity market exerted a positive risk transmission effect on the financial market, while the financial market was able to hedge the risks present in the commodity market.

According to Table 6, before the outbreak of the trade war, $\langle k\rangle = 3.1$, $\langle l\rangle = 6.667$, $\langle m\rangle = 0.52$; after the outbreak of the trade war, $\langle k\rangle = 3.2$, $\langle l\rangle = 6.133$, $\langle m\rangle = 0.76$. The fitting results are shown in Fig. 13.

The fitted parameters obtained before the outbreak of the trade war are:

$$\left[\hat{\beta}_{11}, \hat{\beta}_{22}, \hat{\mu}_1, \hat{\mu}_2, \hat{\beta}_{12}, \hat{\beta}_{21}\right] = [0.0000, 0.4014, 0.1739, 1.0000, -1.5321, 0.9628],$$

and those after the outbreak of the trade war are:

$$\left[\hat{\beta}_{11}, \hat{\beta}_{22}, \hat{\mu}_1, \hat{\mu}_2, \hat{\beta}_{12}, \hat{\beta}_{21}\right] = [0.6973, 0.0000, 0.4132, 1.0000, 1.6193, -2.4350].$$

Before the outbreak of the trade war, the number of infections in the commodity market was generally stable, with the internal infection rate approaching 0 and the external

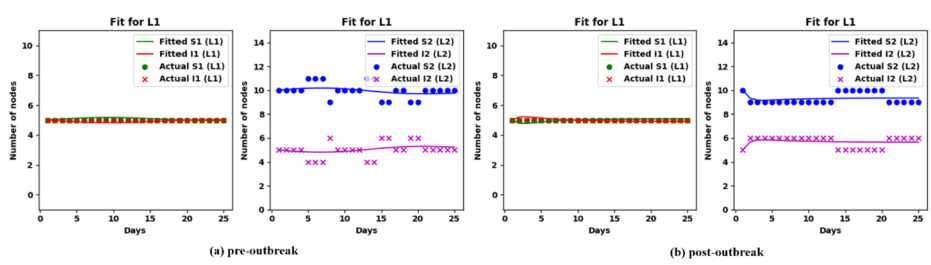

Figure 13 Parameters fitting for the model during the US–China trade war

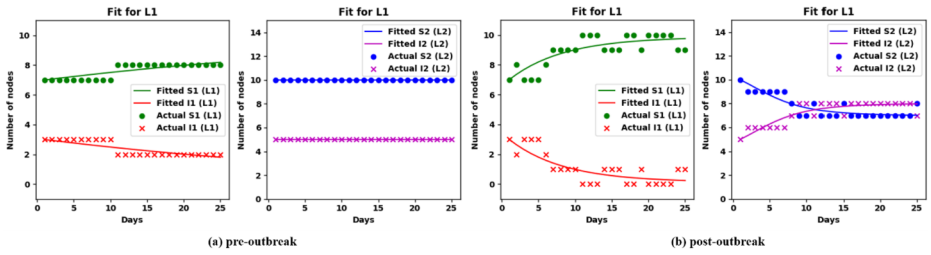

Figure 14 Parameters fitting for the model during the pandemic

transmission rate negative, indicating that it absorbed risk transmission from the financial market. In the financial market, the number of infections fluctuated, with the internal infection rate higher than that of the commodity market and a positive external transmission rate, exacerbating risks in the commodity market. After the outbreak of the trade war, the overall number of infections in the commodity market showed no significant change, but both the internal infection rate and recovery rate in the commodity market increased notably, with a positive external infection rate, indicating that risks from the commodity market could be transmitted to the financial market. The overall number of infections in the financial market exhibited a slight upward trend, with the internal infection rate approaching 0 and absorbing transmission from the commodity market. The external transmission rate was negative, indicating that the financial market was able to hedge against risks from the commodity market at that time.

According to Table 6, before the COVID-19 pandemic, $\langle k \rangle = 2.3$, $\langle l \rangle = 5.4$, $\langle m \rangle = 1.6$;after the outbreak of the pandemic, $\langle k \rangle = 1.6$, $\langle l \rangle = 7.667$, $\langle m \rangle = 0.72$. The fitting results are shown in Fig. 14.

The fitted parameters obtained before the outbreak of the pandemic are:

$$\left[\hat{\beta}_{11}, \hat{\beta}_{22}, \hat{\mu}_1, \hat{\mu}_2, \hat{\beta}_{12}, \hat{\beta}_{21}\right] = [0.0000, 0.0084, 0.0187, 0.0303, 0.0001, -0.0013],$$

and those after the outbreak of the pandemic are:

$$[\hat{\beta}_{11}, \hat{\beta}_{22}, \hat{\mu}_1, \hat{\mu}_2, \hat{\beta}_{12}, \hat{\beta}_{21}] = [0.0000, 0.0859, 0.1308, 0.3050, -0.1693, 0.0043].$$

Before the outbreak of the pandemic, the number of infections in the commodity market exhibited a downward trend, with the internal infection rate approaching 0. In the financial market, the number of infections remained stable, with a certain internal infection rate and recovery rate. The risk transmission rate from the commodity market to the financial market was positive, while the risk transmission rate from the financial market to the commodity market was negative, indicating that the financial market could mitigate some of the risks in the commodity market. Overall, both markets were relatively stable before the pandemic. After the outbreak, the number of infections in the commodity market continued to decline, with the internal infection rate remaining at zero and the external transmission rate turning negative. In contrast, the financial market showed an upward trend in infections, with a slight increase in the internal infection rate compared to the pre-pandemic period and the external transmission rate turning positive. These

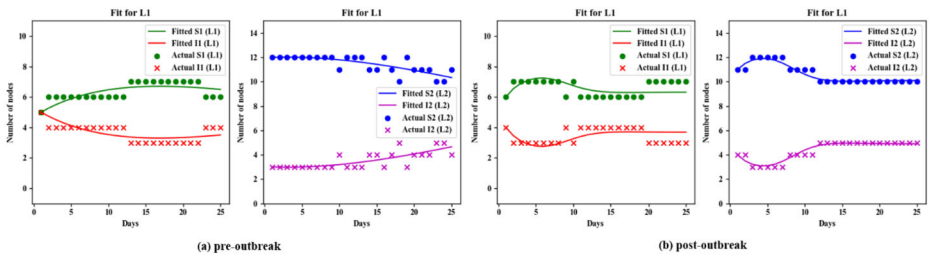

Figure 15 Parameters fitting for the model during the Russia–Ukraine war

changes highlight the commodity market's risk hedging role for the entire financial market.

According to Table 6, before the outbreak of the Russia-Ukraine war, $\langle k \rangle = 3.4$, $\langle l \rangle = 5.6$, $\langle m \rangle = 1.2$; after the outbreak, $\langle k \rangle = 5.2$, $\langle l \rangle = 5.2$, $\langle m \rangle = 0.56$. The fitting results are shown in Fig. 15.

The fitted parameters obtained before the outbreak of the war are:

$$\left[\hat{\beta}_{11}, \hat{\beta}_{22}, \hat{\mu}_1, \hat{\mu}_2, \hat{\beta}_{12}, \hat{\beta}_{21}\right] = [0.0000, 0.0435, 0.0955, 0.1163, -0.0352, 0.1557],$$

and those after the outbreak of the war are:

$$\left[\hat{\beta}_{11}, \hat{\beta}_{22}, \hat{\mu}_1, \hat{\mu}_2, \hat{\beta}_{12}, \hat{\beta}_{21}\right] = [0.0554, 0.0000, 0.0582, 0.0567, 0.1655, -0.4142].$$

Before the outbreak of the Russia–Ukraine war, the number of infections in the commodity market showed a trend of first declining and then rising, with the internal infection rate in the commodity market at 0. The external transmission rate from the financial market was positional contrast, the number of infections on the financial market exhibited an upward trend, with the internal infection rate significantly higher than that of the commodity market, while the external transmission rate from the commodity market was negative, suggesting that the financial market acted as a hedge against risks from the commodity market. After the outbreak of the Russia–Ukraine war, the number of infections in the commodity market showed a trend of first rising and then declining, with an increase in the internal infection rate. The external transmission rate from the financial market turned negative, making the commodity market more receptive to risk hedging from the financial market. In contrast, the number of infections in the financial market displayed an upward trend, with the internal infection rate decreasing towards zero, and the external transmission rate from the commodity market turned positive, indicating that the financial market became more susceptible to transmission from the commodity market.

Before the outbreak of the Russia–Ukraine war, the number of infections in the commodity market showed a trend of first declining and then rising, with the internal infection rate in the commodity market at 0. The external transmission rate from the financial market was positive, indicating that the commodity market absorbed risk transmission from the financial market. In contrast, the number of infections in the financial market exhibited an upward trend, with the internal infection rate significantly higher than that

Table 8 Value of basic reproduction number R_0

	Pre-Bankruptcy	Post-Bankruptcy
R_0	1.7967	3.6570
	Pre-Oil Price Drop	Post-Oil price Drop
R_0	1.4149	1.0946
	Pre-Trade War	After-Trade War
R_0	1.5143	4.0328
	Pre-Pandemic	Post-Pandemic
R_0	1.4940	2.1554
	Pre-War	Post-War
R_0	1.6643	2.5527

of the commodity market, while the external transmission rate from the commodity market was negative, suggesting that the financial market acted as a hedge against risks from the commodity market. After the outbreak of the Russia–Ukraine war, the number of infections in the commodity market showed a trend of first rising and then declining, with an increase in the internal infection rate. The external transmission rate from the financial market turned negative, making the commodity market more receptive to risk hedging from the financial market. In contrast, the number of infections in the financial market displayed an upward trend, with the internal infection rate decreasing towards zero, and the external transmission rate from the commodity market turned positive, indicating that the financial market became more susceptible to transmission from the commodity market.

5.3 Calculating basic reproduction number

Then we use the equations (16)–(18) to calculate the basic reproduction number R_0 before and after the selected specific time points for these extreme events, see Table 8.

We find that $R_0 > 1$ at all chosen periods, which means that spillover risk has always been highly contagious in the two-layer network. Specifically, R_0 is much higher after the bankruptcy of Lehman Brothers, the outbreak of the trade war between U.S. and China, the outbreak of the pandemic and the Russia–Ukraine war. On the contrary, it fells back slightly after the oil price decline.

In September 2008, just before the bankruptcy, the effects of the subprime crisis had already spread from the real estate market to broader financial markets, leading to the accumulation of systemic risk in the global financial system. Although Lehman Brothers announced financial difficulties in August, the market generally overestimated the likelihood of government intervention, making its bankruptcy unexpected and causing global financial markets to rapidly plunge into panic.

In February 2018, prior to the trade war, the global commodity and financial markets were already exhibiting considerable turbulence, with sharp corrections in the U.S. stock market and significant downward pressure in the crude oil and industrial metals markets, indicating that the financial system had accumulated a certain level of risk transmission capacity. In March 2018, the U.S. imposed tariffs on imported steel and aluminum products from China, a move that took the market by surprise, leading to declines in global stock markets and heightened volatility in the commodity markets, further increasing the overall risk transmission capacity of the system. This results in a significant increase in R_0. Similarly, after the outbreak of the pandemic and the Russia–Ukraine war, R_0 also increases rapidly.

It is worth noting that, R_0 decreases slightly after oil crisis. The possible reason is oil prices had been rising steadily before mid-June 2014, with substantial speculative activity in the market, leading prices to deviate from the fundamentals of supply and demand. Following the price drop, speculative funds withdrew, and market bubbles were quickly deflated, causing the commodity market to gradually return to its fundamentals, thereby reducing the overall vulnerability of the market.

In summary, we think that the short-term fluctuations of the basic reproduction number R_0 before and after extreme events are related to the nature of those events. If the event affects a large area and is more sudden and the market is unprepared, then R_0 usually increases following the event. Conversely, if the event is a local and occurs during a period of accumulated risk and the market has expectations about it, then R_0 decreases after the event.

We also find, in the entire system, prior to extreme events, the internal risk transmission rate in financial markets is generally higher than that in commodity markets. The commodity markets are more susceptible to risk transmission from financial markets. After extreme events occur, the internal risk transmission rate in financial markets tends to increase in most cases. However, if an event causes a systemic shock to the commodity market, such as a decline in oil prices or the outbreak of a trade war, the internal transmission rate within the commodity market can increase significantly, while the internal transmission rate in the financial market may decline substantially.

6 Conclusion and discussion

In this paper, a two-layer spillover network for global financial markets and commodity markets is constructed using the standard LASSO-VAR model. Based the network, we discuss the average static spillover risk among the markets over the entire sample period. Then we analyze the dynamic spillover risk of different countries and commodities using the sliding window method. Moreover, we propose an SIS epidemic model to describe the risk contagion procession in the global financial and commodity markets. We select five extreme events and fit the model with actual data of about one month before and after the events. The fitting effect is good. It is worth noting, in these models, the cross-contagion rate parameters between two markets can be positive or negative, indicating that the risks between financial markets and commodity markets can both infect and hedge each other. This reflects the unique nature of financial risk contagion. Finally, we calculate the basic reproduction numbers during different extreme events to reflect the change of risk contagion ability of the system before and after the occurrence of extreme events. The results obtained in this paper provide a new perspective to understand the dynamics propagation process of spillover risk among global financial and commodity markets in the context of connectivity.

Appendix A

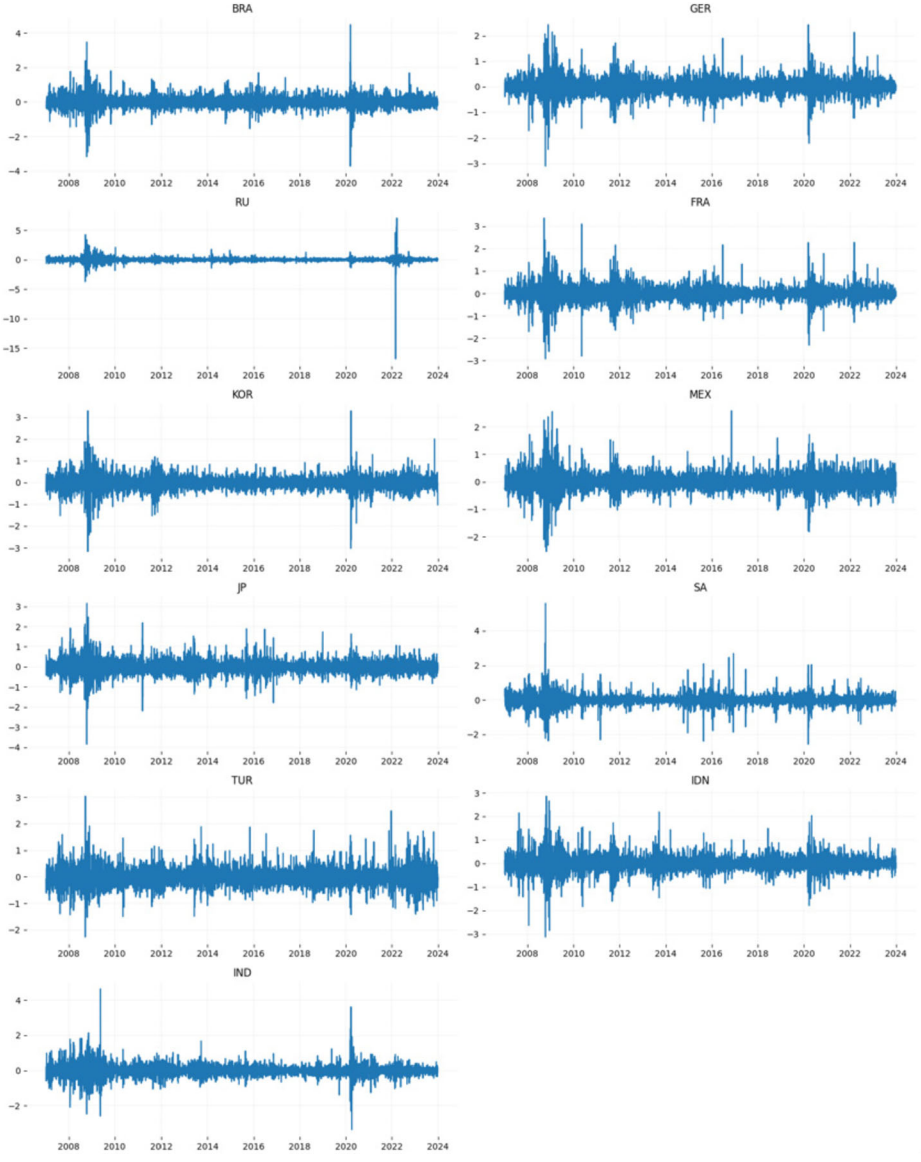

Figure 1 (continued) First difference of financial stress index (FSI) for countries

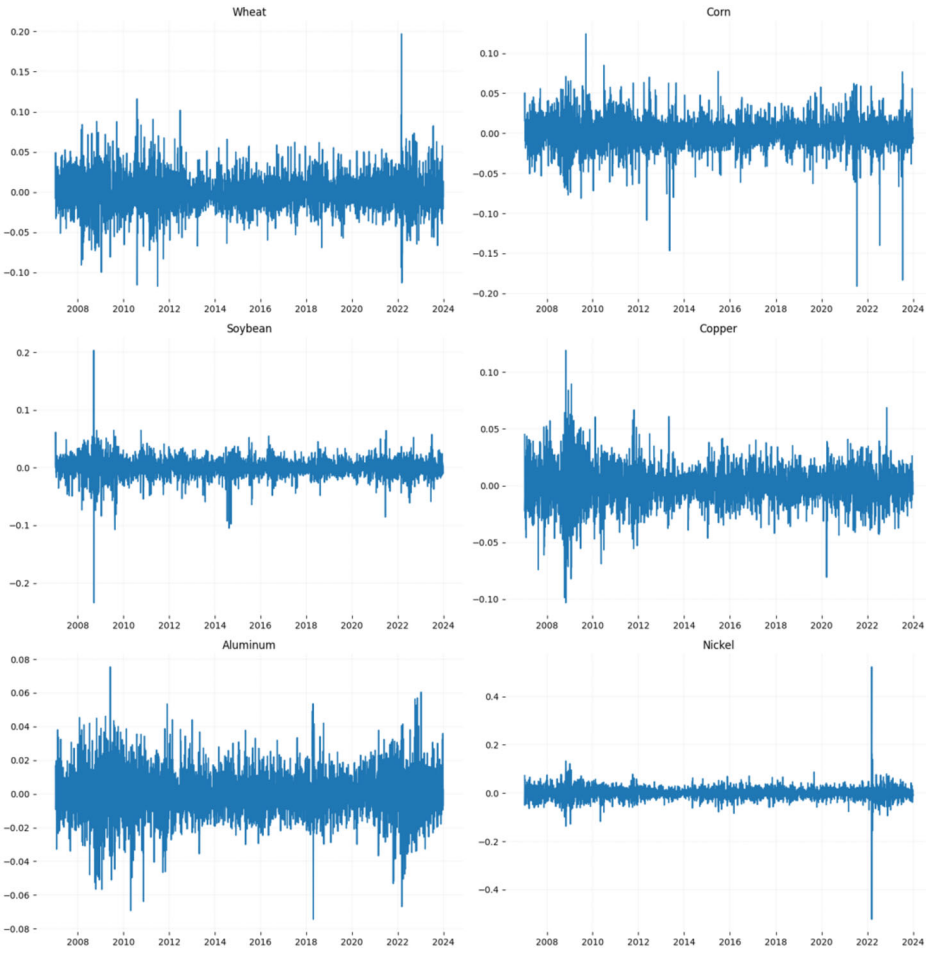

Figure 2 (continued) Logarithmic returns of commodity prices of oil, natural gas, gold, and silver prices

Appendix B

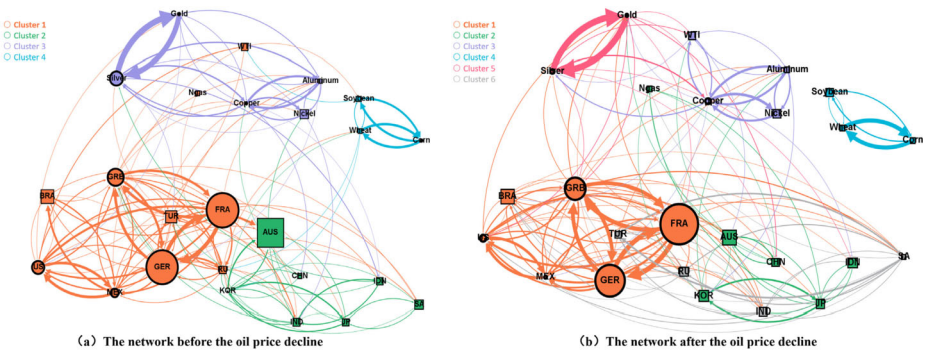

Figure 16 Two-layer networks before and after the oil price decline. *Note:* The network is constructed based on the LASSO-VAR model. Node shapes indicate net spillover status: circles for positive and squares for negative spillover. Node size is proportional to spillover strength, and color represents the cluster. Edge thickness reflects the directional spillover intensity

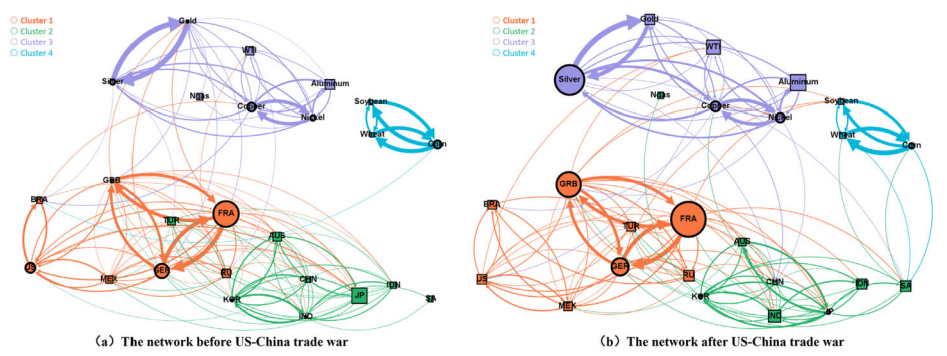

Figure 17 Two-layer networks before and after US–China trade war. *Note:* The network is constructed based on the LASSO-VAR model. Node shapes indicate net spillover status: circles for positive and squares for negative spillover. Node size is proportional to spillover strength, and color represents the cluster. Edge thickness reflects the directional spillover intensity

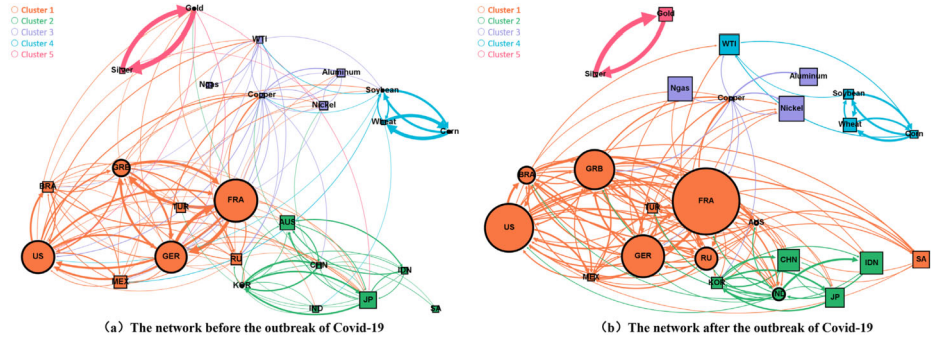

Figure 18 Two-layer networks before and after the outbreak of Covid-19. *Note:* The network is constructed based on the LASSO-VAR model. Node shapes indicate net spillover status: circles for positive and squares for negative spillover. Node size is proportional to spillover strength, and color represents the cluster. Edge thickness reflects the directional spillover intensity

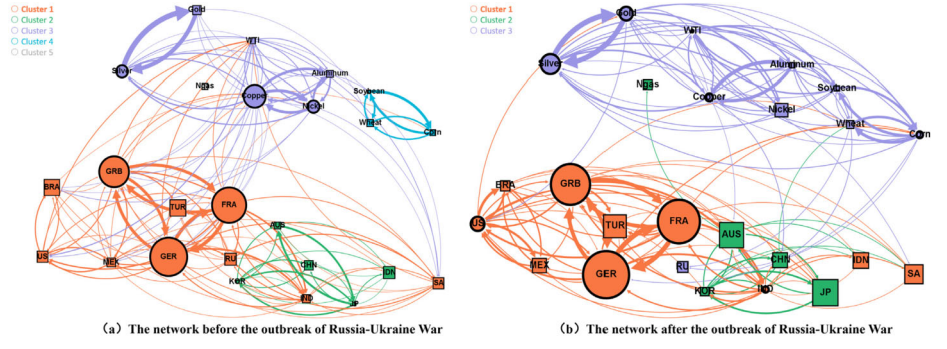

Figure 19 Two-layer networks before and after the outbreak of Russia–Ukraine war. *Note:* The network is constructed based on the LASSO-VAR model. Node shapes indicate net spillover status: circles for positive and squares for negative spillover. Node size is proportional to spillover strength, and color represents the cluster. Edge thickness reflects the directional spillover intensity

Acknowledgements
The authors sincerely thank the editors and anonymous reviewers for their valuable comments and suggestions.

Author contributions
YA: Conceptualization; Formal analysis; Validation; Funding acquisition; Methodology; Supervision; Writing original draft, review and editing. YW: Data curation; Methodology; Software; Validation; Visualization; Writing original draft. All authors read and approved the final manuscript.

Funding
National Natural Science Foundation of China (Grant Number: 12071302).

Data availability
The data used to support the findings of this study will be made available on request. The data is sourced from the commodities, currencies, and indices sections of *Investing.com*.

Declarations

Competing interests
The authors declare that they have no competing interests.

Received: 17 November 2024 Accepted: 12 January 2025 Published online: 04 February 2025

References

1. Luciana, J., Ivan, P.: Unveiling the dance of commodity prices and the global financial cycle. J. Int. Econ. **150**, 103913 (2024)
2. Adhikari, R., Putnam, K.J.: Financial market stress and commodity returns: a dynamic approach. Commodities **3**(1), 39–61 (2024)
3. Hu, C., Liu, X.: The co-movement between commodity and stock markets on the perspective of funding liquidity. J. Financ. Res. **445**(07), 123–139 (2017)
4. Balcilar, M., Usman, O., Agan, B.: On the connectedness of commodity markets: a critical and selective survey of empirical studies and bibliometric analysis. J. Econ. Surv. **38**(1), 97–136 (2024)
5. Acemoglu, D., Ozdaglar, A., Tahbaz-Salehi, A.: Systemic risk and stability in financial networks. Am. Econ. Rev. **105**(2), 564–608 (2015)
6. Adekoya, O.B., Oliyide, J.A., Yaya, O.S., Al-Faryan, M.A.S.: Does oil connect differently with prominent assets during war? Analysis of intra-day data during the Russia-Ukraine saga. Resour. Policy **77**, 102728 (2022)
7. Shahzad, U., Mohammed, K.S., Tiwari, S., Nakonieczny, J., Nesterowicz, R.: Connectedness between geopolitical risk, financial instability indices and precious metals markets: novel findings from Russia Ukraine conflict perspective. Resour. Policy **80**, 103190 (2023)
8. Lin, Z.-L., Ouyang, W.-P., Yu, Q.-R.: Risk spillover effects of the Israel-Hamas War on global financial and commodity markets: a time-frequency and network analysis. Finance Res. Lett. **66**, 105618 (2024)
9. Izzeldin, M., Muradoğlu, Y.G., Pappas, V., Petropoulou, A., Sivaprasad, S.: The impact of the Russian-Ukrainian war on global financial markets. Int. Rev. Financ. Anal. **87**, 102598 (2023)
10. Maggi, M., Torrente, M.-L., Uberti, P.: Proper measures of connectedness. Ann. Finance **16**(4), 547–571 (2020)
11. Alquist, R., Bhattarai, S., Coibion, O.: Commodity-price comovement and global economic activity. J. Monet. Econ. **112**, 41–56 (2020)
12. Gomez-Gonzalez, J.E., Hirs-Garzon, J., Uribe, J.M.: Spillovers beyond the variance: exploring the higher order risk linkages between commodity markets and global financial markets. J. Commod. Mark. **28**, 100258 (2022)
13. Shao, L., Zhang, H., Chang, S., Wang, Z.: Dynamic connectedness between China's commodity markets and China's sectoral stock markets: a multidimensional analysis. Int. J. Financ. Econ. **29**(1), 903–926 (2024)
14. Luo, C., Qu, Y., Su, Y., Dong, L.: Risk spillover from international crude oil markets to China's financial markets: evidence from extreme events and US monetary policy. N. Am. J. Econ. Finance **70**, 102041 (2024)
15. Paul, M., Bhanja, N., Dar, A.B.: Gold, gold mining stocks and equities-partial wavelet coherence evidence from developed countries. Resour. Policy **62**, 378–384 (2019)
16. Malhotra, G., Yadav, M.P., Tandon, P., Sinha, N.: An investigation on dynamic connectedness of commodity market with financial market during the Russia–Ukraine invasion. Benchmarking **31**(2), 439–465 (2024)
17. Umar, M., Farid, S., Naeem, M.A.: Time-frequency connectedness among clean-energy stocks and fossil fuel markets: comparison between financial, oil and pandemic crisis. Energy **240**, 122702 (2022)
18. Diebold, F.X., Yılmaz, K.: On the network topology of variance decompositions: measuring the connectedness of financial firms. J. Econom. **182**(1), 119–134 (2014)
19. Li, Y., Zhuang, X., Wang, J.: Analysis of the cross-region risk contagion effect in stock market based on volatility spillover networks: evidence from China. N. Am. J. Econ. Finance **56**, 101359 (2021)
20. Wang, G.-J., Wan, L., Feng, Y., Xie, C., Uddin, G.S., Zhu, Y.: Interconnected multi-layer networks: quantifying connectedness among global stock and foreign exchange markets. Int. Rev. Financ. Anal. **86**, 102518 (2023)
21. Poledna, S., Molina-Borboa, J.L., Martínez-Jaramillo, S., Van Der Leij, M., Thurner, S.: The multi-layer network nature of systemic risk and its implications for the costs of financial crises. J. Financ. Stab. **20**, 70–81 (2015)
22. Li, S., Wen, S.: Multiplex networks of the guarantee market: evidence from China. Complexity **2017** (2017)
23. Wu, F., Xiao, X., Zhou, X., Zhang, D., Ji, Q.: Complex risk contagions among large international energy firms: a multi-layer network analysis. Energy Econ. **114**, 106271 (2022)
24. Acikgoz, T., Gokten, S., Soylu, A.B.: Multifractal detrended cross-correlations between green bonds and commodity markets: an exploration of the complex connections between green finance and commodities from the econophysics perspective. Fractal Fract. **8**(2), 117 (2024)
25. Biondo, A.E., Pluchino, A., Rapisarda, A.: Informative contagion dynamics in a multi-layer network model of financial markets. Ital. Econ. J. **3**, 343–366 (2017)

26. Chen, N., Fan, H.: Contagion and supervision of liquidity crisis in interbank markets: based on the SIS network model. Phys. A, Stat. Mech. Appl. **629**, 129216 (2023)
27. Huang, Q.-A., Zhao, J.-C., Wu, X.-Q.: Financial risk propagation between Chinese and American stock markets based on multi-layer networks. Phys. A, Stat. Mech. Appl. **586**, 126445 (2022)
28. Balcilar, M., Elsayed, A.H., Hammoudeh, S.: Financial connectedness and risk transmission among MENA countries: evidence from connectedness network and clustering analysis. J. Int. Financ. Mark. Inst. Money **82**, 101656 (2023)
29. Boungou, W., Yatié, A.: Uncertainty, stock and commodity prices during the Ukraine-Russia war. Policy Stud. **45**(3–4), 336–352 (2024)
30. Ngepah, N., da Silva, M.L.A., Saba, C.S.: The impact of commodity price shocks on banking system stability in developing countries. Economies **10**(4), 91 (2022)
31. Illing, M., Liu, Y.: Measuring financial stress in a developed country: an application to Canada. J. Financ. Stab. **2**(3), 243–265 (2006)
32. Mensi, W., Ahmadian-Yazdi, F., Al-Kharusi, S., Roudari, S., Kang, S.H.: Extreme connectedness across Chinese stock and commodity futures markets. Res. Int. Bus. Finance **70**, 102299 (2024)
33. Umar, M., Riaz, Y., Yousaf, I.: Impact of Russian-Ukraine war on clean energy, conventional energy, and metal markets: evidence from event study approach. Resour. Policy **79**, 102966 (2022)
34. Diebold, F.X., Yilmaz, K.: Better to give than to receive: predictive directional measurement of volatility spillovers. Int. J. Forecast. **28**(1), 57–66 (2012)
35. Apostolakis, G., Papadopoulos, A.P.: Financial stress spillovers across the banking, securities and foreign exchange markets. J. Financ. Stab. **19**, 1–21 (2015)
36. Elsayed, A.H., Yarovaya, L.: Financial stress dynamics in the MENA region: evidence from the Arab Spring. J. Int. Financ. Mark. Inst. Money **62**, 20–34 (2019)
37. Nicholson, W.B., Matteson, D.S., Bien, J.: VARX-L: structured regularization for large vector autoregressions with exogenous variables. Int. J. Forecast. **33**(3), 627–651 (2017)
38. Yang, L., Yang, J.: The risk spillover effect of international commodity price fluctuations on China's financial market—a network perspective of volatility spillover. J. Financ. Res. **128**(08), 58–77 (2022)
39. Kang, S.H., McIver, R., Yoon, S.-M.: Modeling time-varying correlations in volatility between BRICS and commodity markets. Emerg. Mark. Financ. Trade **52**(7), 1698–1723 (2016)
40. Pellis, L., Ball, F., Trapman, P.: Reproduction numbers for epidemic models with households and other social structures. I. Definition and calculation of R0. Math. Biosci. **235**(1), 85–97 (2012)
41. Van den Driessche, P., Watmough, J.: Reproduction numbers and sub-threshold endemic equilibria for compartmental models of disease transmission. Math. Biosci. **180**(1–2), 29–48 (2002)
42. Blondel, V.D., Guillaume, J.-L., Lambiotte, R., Lefebvre, E.: Fast unfolding of communities in large networks. J. Stat. Mech. Theory Exp. **2008**(10), P10008 (2008)

Publisher's Note